Available online at www.sciencedirect.com
ScienceDirect
Physica C 456 (2007) 75–82
PHYSICA C
www.elsevier.com/locate/physc

Review

Multi-gap superconductivity in MgB_2: Magneto-Raman spectroscopy

G. Blumberg [a,*], A. Mialitsin [a,1], B.S. Dennis [a], N.D. Zhigadlo [b], J. Karpinski [b]

[a] *Bell Laboratories, Alcatel-Lucent, Murray Hill, NJ 07974, USA*
[b] *Solid State Physics Laboratory, ETH, CH-8093 Zürich, Switzerland*

Received 22 January 2007; received in revised form 10 February 2007; accepted 11 February 2007
Available online 25 February 2007

Abstract

Electronic Raman scattering studies on MgB_2 single crystals as a function of excitation and polarization have revealed three distinct superconducting features: a clean gap below 37 cm^{-1} and two coherence peaks at 109 and 78 cm^{-1} which we identify as the superconducting gaps in π- and σ-bands and as the Leggett's collective mode arising from the fluctuation in the relative phase between two superconducting condensates residing on corresponding bands. The temperature and field dependencies of the superconducting features have been established. A phononic Raman scattering study of the E_{2g} boron stretching mode anharmonicity and of superconductivity induced self-energy effects is presented. We show that anharmonic two phonon decay is mainly responsible for the unusually large linewidth of the E_{2g} mode. We observe ~2.5% hardening of the E_{2g} phonon frequency upon cooling into the superconducting state and estimate the electron–phonon coupling strength associated with this renormalization.

Keywords: Superconductivity; Raman spectroscopy

Contents

* Corresponding author. Tel.: +1 908 582 6983.
E-mail address: girsh@bell-labs.com (G. Blumberg).
[1] Department of Physics and Astronomy, Rutgers University, Piscataway, NJ 08854, USA.

0921-4534/$ - see front matter © 2007 Elsevier B.V. All rights reserved.
doi:10.1016/j.physc.2007.02.011

1. Introduction

The multi-gap nature of superconductivity in MgB_2 was predicted theoretically [1] and has been experimentally established by a number of spectroscopies. A double-gap structure in the quasiparticle energy spectra was determined from tunneling spectroscopy [2,3]. The two gaps have been assigned to distinctive quasi-two-dimensional σ-bonding states of the boron $p_{x,y}$ orbitals and three-dimensional π-states of the boron p_z orbitals Fermi surface (FS) sheets by means of ARPES [4,5]: $\Delta_\sigma = 5.5$–6.5 and $\Delta_\pi = 1.5$–2.2 meV. Scanning tunneling microscopy (STM) has provided a reliable fit for the smaller gap, $\Delta_\pi = 2.2$ meV [6]. This value manifests in the absorption threshold energy at 31 cm^{-1} obtained from magneto-optical far-IR studies [7]. The nominal upper critical field H_{c2}^{π} deduced from the coherence length $\xi_\pi = 49.6$ nm by vortex imaging is $H_{c2}^{\pi} \approx 0.13$ T [6] which is much smaller than the critical field $H_{c2}^{opt} \approx 5$ T found by magneto-optical measurements [7].

Electronic Raman studies on MgB_2 have explored the superconducting (SC) energy gap and changes in phonon lineshapes, starting with the work of [8,9] and followed thereafter by [10,11]. The dependence of the Raman response on scattering geometry allowed an observation of the pairing gap on the two-dimensional σ-bands and the 3D π-bands. By orienting the light polarizations along the *c*-axis of MgB_2 (perpendicular to the hexagonal planes) the weakly dispersing σ-bands cannot be probed and thus only the π-bands are projected out, giving an observed threshold at $2\Delta_\pi = 29$ cm^{-1} [11]. The larger $2\Delta_\sigma$ gap has been demonstrated by Raman experiments as a SC coherence peak at 105 cm^{-1} [10].

For multi-band superconductors collective modes associated with fluctuations of the relative phase and amplitudes of coupled condensates [12–14] as well as distinctive self-energy effects associated with intra- and inter-band interactions [1,15] were expected. It has been suggested from STM vortex imaging that the superconductivity in the π-band is induced by superconductivity in the σ-band [6], however, the coupling mechanism remained unclear. Previous phononic Raman spectroscopy has identified a broad Γ-point phonon centered around 620–640 cm^{-1} [8–10] consistent with the calculated frequency of the anharmonic E_{2g} boron stretching mode [15,16]. The phononic dispersion has been studied by inelastic X-ray scattering [17,18]. However, the expected self-energy effects [1,15] have not been demonstrated.

1.1. Experimental

Polarized Raman scattering can probe excitations around the Brillouin zone (BZ) center that belong to different symmetry representations within the space group of the crystal structure. The point group associated with MgB_2 is D_{6h}. We denote by ($\mathbf{e}_{in}$ $\mathbf{e}_{out}$) a configuration in which the incoming/outgoing photons are polarized along the $\mathbf{e}_{in}$/$\mathbf{e}_{out}$ directions. The vertical (V) or horizontal (H) directions were chosen perpendicular or parallel to the crystallographic *a*-axis. The "right–right" (RR) and "right–left" (RL) notations refer to circular polarizations: $\mathbf{e}_{in} = (H - iV)/\sqrt{2}$, with $\mathbf{e}_{out} = \mathbf{e}_{in}$ for the RR and $\mathbf{e}_{out} = \mathbf{e}_{in}^*$ for the RL geometry. For the D_{6h} point group the RR and HH polarizations select correspondingly A_{1g} and $A_{1g} + E_{2g}$ symmetries while both RL and VH select the E_{2g} representation.

Raman scattering was performed in back scattering geometry from the *ab* surface of MgB_2 single crystals grown as described in [19] using less than 2 mW of incident power focused to a 100×200 μm spot. The data in magnetic field was acquired with a continuous flow cryostat inserted into the horizontal bore of a SC magnet. The sample temperatures quoted have been corrected for laser heating. We used the excitation lines of a Kr^+ laser and a triple-grating spectrometer for analysis of the scattered light. The data were corrected for the spectral response of the spectrometer and the CCD detector and for the optical properties of the material at different wavelengths as described in Ref. [20].

1.2. Raman response

In Fig. 1 we show the Raman response from an MgB_2 single crystal for the E_{2g} and A_{1g} scattering channels in the normal and SC states. The E_{2g} scattering channel is accessed by RL scattering polarization geometries and the A_{1g} channel by RR geometry.

The response comprises electronic and phononic contributions. The electronic Raman response at low frequencies in the SC state is decomposed into a sum (solid lines) of a gapped normal state continuum with temperature broadened $2\Delta_0 = 37$ cm^{-1} gap cutoff (threshold at 33 cm^{-1}), the SC coherence peak at $2\Delta_l = 109$ cm^{-1} (black solid line), and a novel collective mode at $\omega_L = 76$ cm^{-1} (green solid line). The latter is present only in the A_{1g} scattering channel. To fit the observed shapes the theoretical coherence peak singularity $\chi'' \sim 4\Delta_l^2/(\omega\sqrt{\omega^2 - 4\Delta_l^2})$ is broadened by convolution with a Lorentzian with HWHM = 12% of $2\Delta_l$ for the E_{2g} channel and 20% for the A_{1g} channel. The collective mode ω_L is broadened to HWHM = 18 cm^{-1}.

For the high energy part of the spectra the broad E_{2g}-band *I* centered at about 630–640 cm^{-1} corresponds to the boron stretching mode which is the only Raman active phonon for the MgB_2 structure. It is also the only phononic mode demonstrating renormalization below the SC transition [21]. All the other high frequency modes (II–VI) in the A_{1g} and E_{2g} channels correspond to twice the energy of distinctive flat portions in the phonon dispersions measured by inelastic X-ray scattering [17,18] and we assign them to two phonon scattering. The 'E_{1u}-branch' and a two-fold degenerate low energy acoustic phonon branch have a coinciding minimum in the *A*-point of the BZ thus delivering a large Raman response for the two-phonon peak II. Peak III is due to flat portions of low energy acoustic

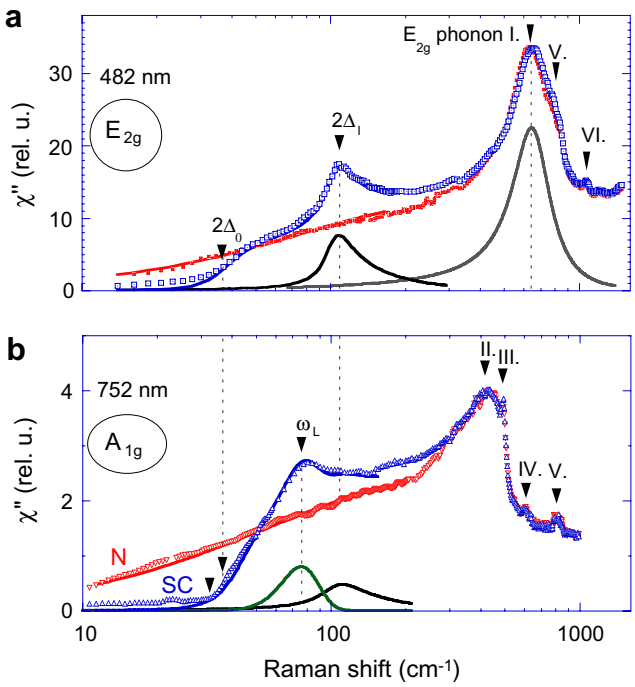

Fig. 1. The Raman response spectra of an MgB_2 crystal in the normal (red) and SC (blue) states for the E_{2g} (top) and A_{1g} (bottom) scattering channels. The data is acquired at 8 K. The normal state has been achieved by applying a 5 T magnetic field parallel to the c-axis. Decomposition into SC coherence peaks, E_{2g} phonon and the fits are shown by solid lines. (For interpretation of the references in colour in this figure legend, the reader is referred to the web version of this article.)

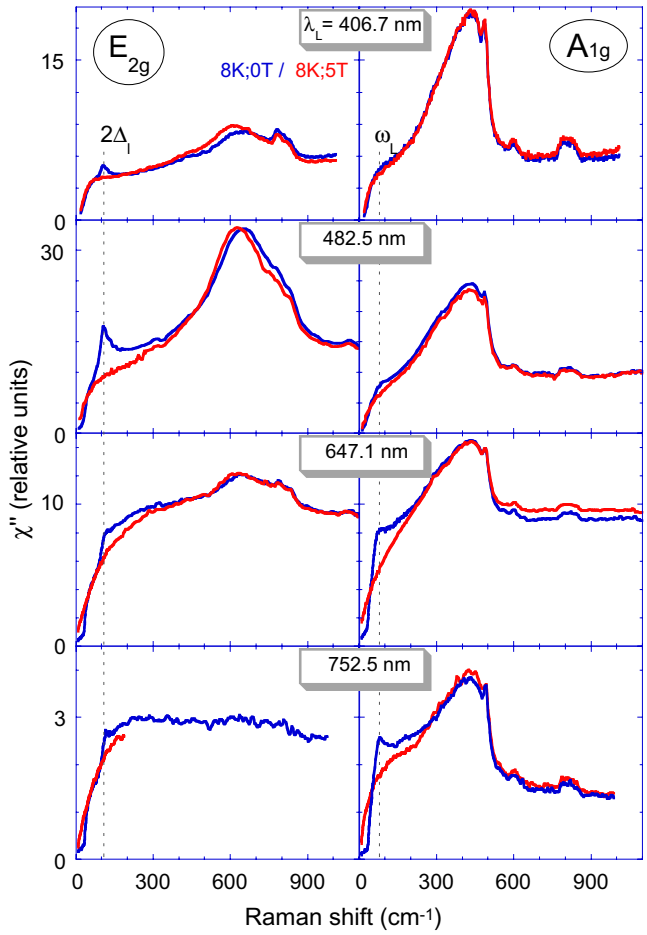

Fig. 2. Raman response function at 8 K in the SC (blue) and normal (red) states for the E_{2g} (RL) and the A_{1g} (RR polarization) scattering channels as a function of excitation wavelengths. (For interpretation of the references in colour in this figure legend, the reader is referred to the web version of this article.)

phonon branches when they approach the M-point. Peak IV is at twice the frequency of a distinctive saddle point of a high energy acoustic phonon branch in A-point. The 'A_{2u} branch' is mostly flat all the way along the Γ–A line at around 400 cm^{-1}. This might explain the peculiar symmetry indifferent behavior of peak V. Finally the E_{2g} optical branch has a minimum in the A-point at about 530 cm^{-1} resulting in the two-phonon scattering peak VI.

1.3. Resonant Raman excitation profile

Light can couple to electronic and phononic excitations *via* resonant or non-resonant Raman processes [22]. The Raman scattering cross-section can be substantially enhanced when the incident photon energy is tuned into resonance with optical inter-band transitions. The resonance Raman excitation profile (RREP) provides information about the scattering probabilities seen in the Raman spectra. For MgB_2 the inter-band contribution to the in-plane optical conductivity $\sigma_{ab}(\omega)$ contains strong IR peaks with a tail extending to the red part of the visible range and a pronounced band around 2.6 eV [23,24] (Fig. 3). The IR peaks are associated with transitions between two σ-bands while the 2.6 eV peak is associated with the $\pi \rightarrow \sigma$ electronic transitions in the vicinity of the Γ-point and $\sigma \rightarrow \pi$ transitions in the vicinity of the M-point of the BZ [15,25,26].

To explore the resonance conditions we analyze Raman spectra as a function of excitation energy. In Fig. 2 we show Raman spectra in the SC and normal states for the E_{2g} and A_{1g} scattering channels for four excitation energies. The normal state has been achieved by applying a 5 T magnetic field parallel to the c-axis. All spectra show a relatively strong electronic Raman continuum that extends beyond our measurement range. The electronic scattering intensity in the fully symmetric A_{1g} channel is not much weaker than in the E_{2g} channel indicating cancellation of screening that could be due to multi-band contributions with opposite sign of the effective mass near the FS [27].

2. Electronic Raman response

The low frequency part of the electronic Raman continuum changes in the SC state (Figs. 1 and 2), reflecting renormalization of electronic excitations resulting in three new features in the spectra: (i) a threshold of Raman intensity at 33 cm^{-1} ($2\Delta_0 = 37$ cm^{-1}), (ii) a SC coherence peak at $2\Delta_1 = 109$ cm^{-1}, and (iii) a new mode at 76 cm^{-1}, which

is in-between the $2\Delta_0$ and $2\Delta_l$ energies. The observed energy scales of the fundamental gap Δ_0 and the large gap Δ_l are consistent with Δ_π and Δ_σ as assigned by one-electron spectroscopies [4–6]. The features (i) and (ii) are seen in all scattering geometries while mode (iii) contributes only to the A_{1g} scattering channel.

The Raman coupling to the $2\Delta_l$ electronic coherence peak in the SC state is provided by density fluctuations in the σ-band. For the E_{2g} channel the peak intensity is enhanced by about an order of magnitude when the excitation photon energy is in resonance with the 2.6 eV $\sigma \rightarrow \pi$ inter-band transitions (Fig. 3). In contrast, for the fully symmetric A_{1g} channel the integrated intensity of the $2\Delta_l$ coherence peak does not follow the optical conductivity and is about five times weaker than for the resonant excitation in the E_{2g} channel. Nonetheless, due to relative charge density fluctuations between two coupled σ- and π-bands the intensity in the fully symmetric channel is only partially screened. The integrated intensity of the ω_L collective mode in the A_{1g} channel shows excitation dependence similar to one for the $2\Delta_l$ coherence peak in the same channel.

2.1. The fundamental gap

At the fundamental gap value $2\Delta_0$ the spectra for all symmetry channels show a threshold without a coherence peak. This threshold appears cleanest for the spectra with lower energy excitations for which the low-frequency contribution of multi-phonon scattering from acoustic branches is suppressed (see Fig. 2). The absence of the coherence peak above the threshold is consistent with the expected behavior for a dirty superconductor [22]. Thus the π-bands show signatures of strong intrinsic scattering leading to the observed Raman continuum.

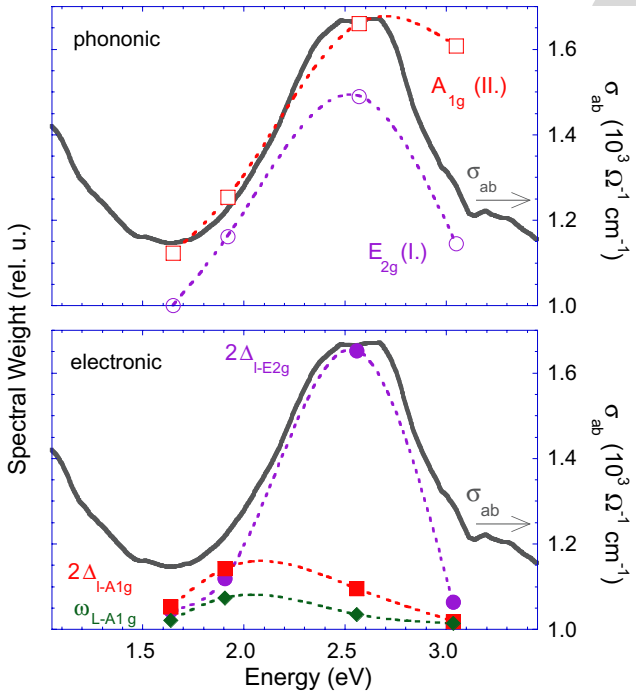

Fig. 3. Comparison of *ab*-plane optical conductivity (Ref. [24]) and resonant Raman excitation profiles for phononic and electronic excitations. The empty symbols show the 340 cm^{-1} A_{1g} and the 640 cm^{-1} E_{2g} phonon intensities and the solid symbols show the SC coherence peaks intensities. All dashed lines are guides for the eye.

The ratio $2\Delta_0/k_BT_c$ is only 1.2 which makes the π-band contribution to the two band superconductivity quite tenuous. That is in agreement with rapid suppression of the threshold by a relatively weak magnetic field applied along the *c*-axis (see Fig. 4d).

2.2. Large gap in σ-bands

The $2\Delta_l$ coherence peak is seen for all scattering geometries. For the E_{2g} channel it appears as a sharp singularity with continuum renormalization extending to high energies, which is in agreement with expected behavior for clean superconductors [22]. The $2\Delta_l$ coherence peak frequency shows a BCS-like temperature dependence with the $2\Delta^E/k_BT_c$ ratio of about 4 indicating a moderately strong coupling limit (see inset in Fig. 5c).

Coulomb screening suppresses the scattering intensity for the fully symmetric A_{1g} channel. The $2\Delta_l$ coherence peak intensity does not follow the optical conductivity. The Raman intensity in the fully symmetric channel is governed by the difference in light coupling to the π- and σ-bands which explains the intensity enhancement seen for the pre-resonant excitations (Fig. 3). Also, the coherence peak in the A_{1g} channel is broader than in the E_{2g} channel due to stronger cross relaxational coupling to the π-band quasiparticles.

2.3. Leggett's collective mode

The novel mode at 76 cm^{-1} contributes only to the A_{1g} scattering channel. This mode is more pronounced for off-resonance excitation for which the electronic continuum above the fundamental threshold $2\Delta_0$ is weaker. We attribute this feature to the collective mode proposed by Leggett [12]: If a system contains two coupled superfluid liquids a simultaneous cross-tunneling of a pair of electrons becomes possible. Leggett's collective mode is caused by dynamic oscillations of Cooper pairs between the two superfluids leading to small fluctuations of the relative phase of two condensates while the total electron density at every spatial point of the superconductor is conserved. Such excitation couples to the A_{1g} Raman scattering channel. If the energy of this mode is below the pair-breaking gap, the mode dissipation is suppressed and the excitation is expected to be long-lived. In the case of MgB_2 the two coupled SC condensates reside at the σ- and π-bands.

The excitation of Leggett's mode is gapped with a dispersion relation for small momentum q given by [12,13,28]

$$\Omega_L(q)^2 = \omega_L^2 + v^2q^2, \quad (1)$$

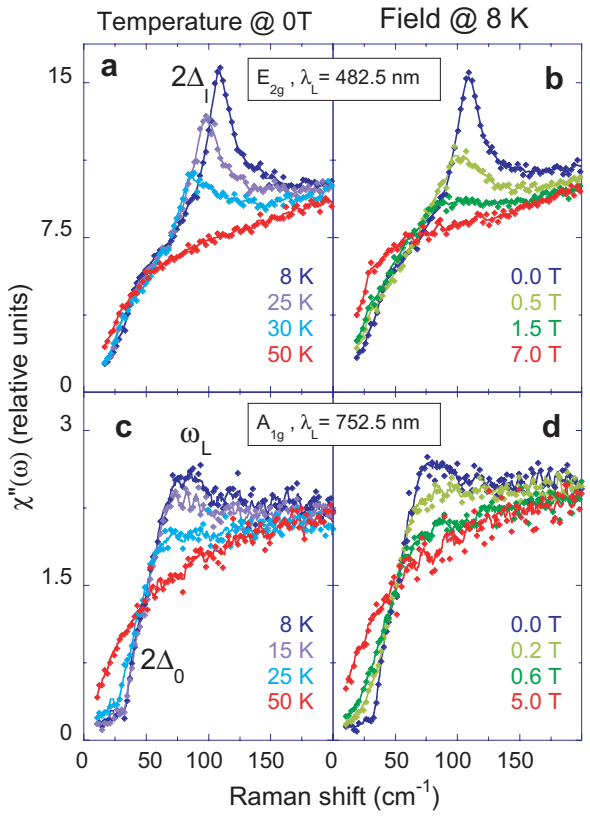

Fig. 4. Evolution of low-frequency Raman response as a function of temperature at zero field and field at 8 K. The E_{2g} scattering channel (RL) with 482.5 nm excitation and the A_{1g} channel (RR) with 752.5 nm excitation are shown.

where in the low frequency limit the excitation gap can be expressed *via* intra- and inter-band pairing potentials $V_{\sigma\sigma}$, $V_{\pi\pi}$ and $V_{\sigma\pi}$, the gaps Δ_σ and Δ_π and the density of states N_σ and N_π in corresponding bands

$$\omega_L^2 = \frac{N_\sigma + N_\pi}{N_\sigma N_\pi} \frac{4V_{\sigma\pi}\Delta_\sigma\Delta_\pi}{V_{\sigma\sigma}V_{\pi\pi} - V_{\sigma\pi}^2}. \quad (2)$$

Leggett's mode exists only if $V_{\sigma\sigma}V_{\pi\pi} > V_{\sigma\pi}^2$. The estimates of the coupling constants by first principal computations [1,15,29] show that for the MgB_2 superconductor this condition is satisfied and the estimate for the mode energy is in between 60 and 85 cm^{-1} which is consistent with the observed mode at 76 cm^{-1}. Because the collective mode energy is in between the two-particle excitation thresholds for the π- and σ-bands, $2\Delta_\pi < \omega_L < 2\Delta_\sigma$, Leggett's excitation rapidly relaxes into π-band quasiparticles. Indeed, the measured Q-factor for this mode is about two: the Cooper pair tunneling energy relaxes into π-band quasiparticle continuum within a couple of tunneling oscillations. Despite being short lived, Leggett's mode in MgB_2 couples to light and is observed by Raman spectroscopy.

2.4. Effects of temperature and field

In Fig. 4 the evolution of the $2\Delta_l$ coherence peak and Leggett's collective mode ω_L across the SC transition is displayed for two cases: varying temperature at zero magnetic field (a, c) and varying magnetic field at 8 K (b, d). The coherence peaks lose their intensity and move to lower energies by either increasing temperature or field. The intensity threshold $2\Delta_0$ is already smeared out at magnetic fields as weak as 0.2 T, consistent with H_{c2}^{π} deducted from vortex imaging [6]. Leggett's collective mode ω_L persists up to 0.6 T while the SC coherence peak $2\Delta_l$ is suppressed beyond 2 T. $2\Delta_l(T,H)$ is shown in the insets of Fig. 5. It exhibits a BCS-like temperature dependence and a linear reduction in field with a rapid slope of about -15 cm^{-1}/T. A linear extrapolation for the $2\Delta_l$ gap collapse leads to 7 T, a field that is higher than H_{c2}^{opt} [7], while the coherence peak intensity survives only up to 2 T.

3. Phononic Raman response

High-T_c superconductivity in MgB_2 is known to be promoted mainly due to the boron layers [26], thus the high frequency lattice vibrations of light boron atoms beneficially increase the electron–phonon coupling. The E_{2g} Raman active in-plane boron vibrational mode contributes significantly to superconductivity; this fact is reflected by

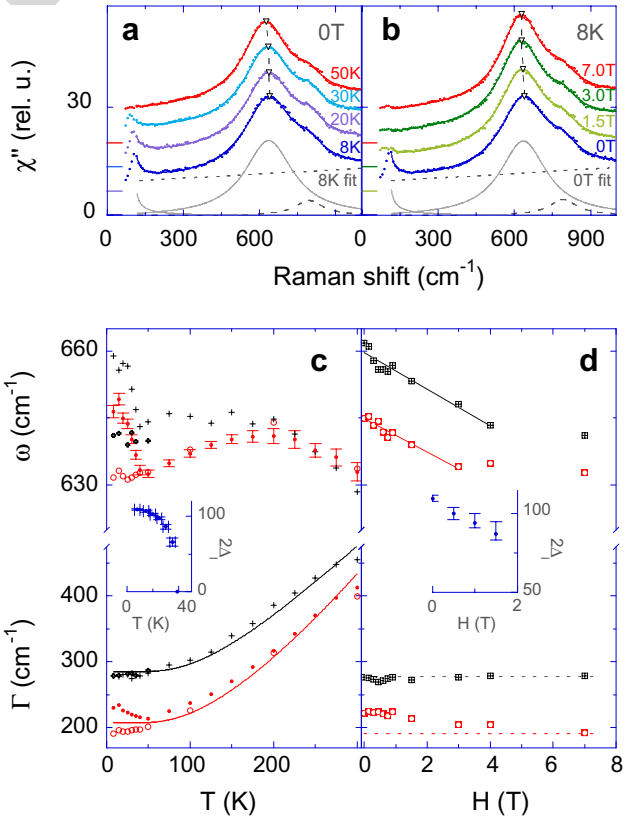

Fig. 5. Evolution of the E_{2g} phonon with temperature (a) and field (b) using 482.5 nm excitation and (RL) polarization. The phonon frequency $\omega(T,H)$ and the damping constant $\Gamma(T,H)$ are drawn as functions of temperature (c) and field (d) for two crystals $\mathscr{A}$ (black) and $\mathscr{B}$ (red symbols). Insets show temperature and field dependencies of the $2\Delta_l$ energy. (For interpretation of the references in colour in this figure legend, the reader is referred to the web version of this article.)

the Eliashberg function $\alpha^2F(\omega)$ peaking in the same frequency range where a high phononic density of states is accounted for by Van Hove singularities of the E_{2g} branch in the Γ and A-points of the BZ [16,30]. The reason the E_{2g} mode plays a prominent role in the SC mechanism is that the mode strongly couples to the σ-type states of the boron plane as can be seen from the basic geometry of the electronic configuration [29].

Raman spectra exhibit an unusually broad linewidth of the E_{2g} boron stretching mode [9,10,21,31] which has been the subject of numerous speculations. While high impurity scattering in earlier low quality samples has been suggested as one of the possible reasons, this mechanism can be readily excluded with recent high quality single crystals. The two remaining contributions to the E_{2g} phonon rapid decay are (i) strong electron–phonon coupling and (ii) multi-phononic decay (subsequently referred to as *anharmonicity*). The relative importance of the electron–phonon coupling and anharmonicity in this matter is still under debate. On one hand a density functional theory calculation asserts that the anharmonic contribution to the E_{2g} phonon linewidth is negligible ($\sim$10 cm^{-1}) [17]. On the other hand analysis of the phonon self-energy in the long wavelength limit shows that the σ-band contribution to the phonon decay is vanishing [32]. Thus, even when contributions of the spectral weight of $\alpha^2F(\omega)|_{\omega<\omega_{E_{2g}}}$ to the damping of the E_{2g} phonon are accounted for [33], the experimentally observed linewidth of 200–280 cm^{-1} at low temperatures [10,21,31] cannot be explained with electron–phonon coupling alone whose part in the E_{2g} mode linewidth at low temperatures amounts to about 50 cm^{-1} even in such an elaborate scenario as that in Ref. [33].

Raman scattering experiments have shown that the frequency of the E_{2g} mode in single crystals at room temperature is around 635 cm^{-1} [10,21,31] whereas theoretical calculations systematically underestimate this value by about 80 cm^{-1} [16,17]. It has been suggested that if the E_{2g} band around the Γ-point is anharmonic then the E_{2g} mode frequency is increased by the missing amount to match the experimentally observed value [1,34]. In addition, the experimentally observed T_c and the reduced isotope effect [35] can only be reconciled within anisotropic strong coupling theory if the E_{2g} mode anharmonicity is explicitly included [29,36].

3.1. Excitation dependence

The Raman intensities for phononic modes are in resonance with the 2.6 eV optical transitions. The resonance is more distinct for the E_{2g} phonon mode that reduces by an order of magnitude for adjacent violet and red excitations and almost vanishes in the infra-red (see Fig. 3) inferring that the Raman coupling to this phonon is realized only via $\pi \leftrightarrow \sigma$ inter-band transitions. In contrast, the two-phonon scattering in the A_{1g} channel remains visible even for pre-resonance excitations.

3.2. Dependence on temperature and field

In Fig. 5a and b we show the temperature dependence of the E_{2g} Raman response measured on cooling in zero field and as a function of field at 8 K. The data (dots) are fitted with two phononic oscillators and a SC coherence peak (solid lines) on an electronic continuum (decompositions for the lowest spectra are shown). In Fig. 5c and d we evaluate the temperature and field dependencies of the E_{2g} phonon frequency $\omega(T,H)$ and the damping constant $\Gamma(T,H)$ for two crystals $\mathscr{A}$ and $\mathscr{B}$ where we distinguish between the respective values for the SC and normal states measured at zero field cooling (solid symbols) and 8 T cooling (empty symbols). The solid line in Fig. 3 is a fit of the damping constant $\Gamma(T)$ in the normal state to a model of anharmonic two and three phonon decay at one-half and one-third frequencies:

$$\Gamma(T) = \Gamma_0 + \Gamma_3[1 + 2n(\Omega(T)/2)] + \Gamma_4[1 + 3n(\Omega(T)/3) + 3n^2(\Omega(T)/3)]. \quad (3)$$

Here $\Omega(T) = hc\omega_h/k_BT$, with the harmonic frequency $\omega_h = 540$ cm^{-1} [15,17,26], $n(x)$ is the Bose–Einstein distribution function, Γ_0 is the internal temperature independent linewidth of the phonon, and $\Gamma_{3,4}$ are broadening coefficients due to the cubic and quartic anharmonicity. The results of the fit to this anharmonic decay model are collected in Table 1. For both crystals the broadening coefficients $\Gamma_3 + \Gamma_4 \gg \Gamma_0$ and therefore the anharmonic decay is primarily responsible for the large damping constant of the E_{2g} phonon. We identify the reason for this rapid phononic decay in the phononic density of states (PDOS) peaking at 265 cm^{-1}, half of the harmonic E_{2g} phonon frequency ω_h (Refs. [16,37]), which corresponds to the Van-Hove singularity of the lower acoustic branch, almost dispersionless along the Γ–K–M direction. In this context the narrowing of the E_{2g} mode with Al substitution observed in Refs. [31,38] can be readily explained with the E_{2g} phonon branch moving to energies above 100 meV with increased Al concentration whereas the acoustic modes that provide the decay channels stay close to their original energies with high PDOS in the energy range of 200–320 cm^{-1} [38]. In short, the fast decay of the E_{2g} mode is due to the unique combination of its harmonic frequency in the Γ-point corresponding to high PDOS at half of this frequency. The residual linewidth Γ_0 that we obtain from the fit to the anharmonic decay model, while small, is

Table 1
Comparison of T_c and the E_{2g} oscillator parameters for crystals $\mathscr{A}$ and $\mathscr{B}$

Crystal	T_c (K)	ω_0^N (cm^{-1})	ω_0^{SC} (cm^{-1})	Γ_0 (cm^{-1})	Γ_3 (cm^{-1})	Γ_4 (cm^{-1})	κ (%)
$\mathscr{A}$	38.2	640	659	32 ± 12	253 ± 10	small	3
$\mathscr{B}$	38.5	630	649	small	185 ± 6	23 ± 3	3

not in contradiction with the theoretical estimates [32,33] of the electron–phonon decay contribution to the E_{2g} phonon linewidth.

It is worth noting that individual Γ_i parameters differ for the two single crystals despite the fact that both samples were grown in the same batch. The E_{2g} mode for crystal $\mathscr{A}$ is broader by about 10 meV than for crystal $\mathscr{B}$. With $\Gamma_0^{\mathscr{A}}$ somewhat higher than $\Gamma_0^{\mathscr{B}}$ and $\Gamma_3^{\mathscr{A}}$ substantially higher than $\Gamma_3^{\mathscr{B}}$ (see Table 1) the E_{2g} mode in crystal $\mathscr{A}$ is more anharmonic than in crystal $\mathscr{B}$. Accordingly the crystal $\mathscr{A}$ mode is pushed to about 10 cm^{-1} higher frequency at low temperatures. We note a correlation between the larger anharmonicity and slightly lower T_c in the case of crystal $\mathscr{A}$.

3.3. Pressure and Al substitution

The boron stretching E_{2g} phonon has been found to be the most sensitive mode to structural changes upon substitution of Mg sites with Al. The Raman spectra of gradual substitution $Al_xMg_{1-x}B_2$ are quite complicated with non-uniform transfer of spectral weight from the 640 cm^{-1} mode as observed in pure MgB_2 to the 980 cm^{-1} AlB_2 E_{2g} mode [31]. Upon complete substitution the change in shape and frequency is striking as the E_{2g} mode in AlB_2 has stiffened more than 300 cm^{-1} and its line width has narrowed from 400 cm^{-1} to about 50 cm^{-1} (see Fig. 6a). With Al substitution the large anharmonicity of the E_{2g} phonon mode is reduced.

The pressure dependence of the E_{2g} phonon frequency links its frequency shift to the variation of the lattice parameters [9]. In the pressure range up to 15 GPa the mode frequency shifts linearly with pressure (Fig. 6b). An unusually large Grüeneisen parameter of 3.9 has been deduced from this frequency shift [39]. The larger Grüeneisen parameters are usually related to increased anharmonicity of the mode [40] which fits in the overall picture of anharmonicity as discussed above. Also interesting is the link to the linear decrease of T_c with pressure [41,42].

The temperature dependence between room temperature and T_c is a smooth but nonmonotonic function peaking at 200 K (fit results to the spectra are shown in Fig. 5c). Its particular functional shape reflects the variation of anharmonicity of the E_{2g} mode as a function of temperature as both the E_{2g} band and the corresponding decay channels react to lattice expansion with increased temperature.

3.4. Phononic self-energy effects

To describe the superconductivity induced self-energy effect we refer to Fig. 5c. Upon cooling in zero field the E_{2g} phonon frequency exhibits nonmonotonic but smooth behavior down to T_c. Then at T_c it displays abrupt hardening with $\omega_0^{SC}(T)$ scaling to the functional form of the SC gap magnitude $2\Delta_I(T)$. For in-field cooling the E_{2g} phonon frequency $\omega_0^N(T)$ remains unrenormalized. The differences

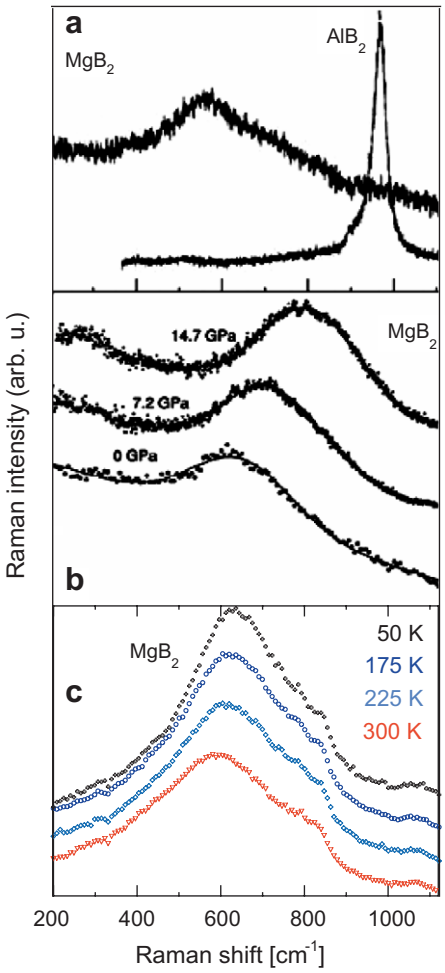

Fig. 6. The phononic Raman intensity in E_{2g} channel as function of substitution, pressure and temperature. (a) MgB_2 vs. AlB_2 at room temperature from Ref. [38]. (b) The pressure dependence from Ref. [9]. (c) The temperature dependence at ambient pressure. Spectra are shifted vertically for clarity.

between the phonon frequencies in the normal and SC states at 8 K are 19 ± 3 cm^{-1} for both crystals $\mathscr{A}$ and $\mathscr{B}$. To quantify the relative hardening of the E_{2g} mode we obtain the superconductivity induced renormalization constant $\kappa = (\omega_0^{SC}/\omega_0^N) - 1 \approx 3\%$ (see Table 1) which is much smaller than the theoretically predicted $\kappa \approx 12\%$ [1].

We estimate the electron–phonon coupling constant $\lambda_{E_{2g}}^{\Gamma}$ around the BZ center using approximations adopted in Refs. [43,44]: $\lambda = -\kappa \mathscr{R}e(\frac{\sin u}{u})$, where $u \equiv \pi + 2i \times \cosh^{-1}(\omega^N/2\Delta_\sigma)$, and obtain $\lambda_{E_{2g}}^{\Gamma} \approx 0.3$. This estimate of the coupling constant is consistent with the fit to a phenomenological model [45] where the direct coupling of light to the σ-bands is neglected but it is smaller than the values predicted by the first principal computations [1,15,26,29,46].

We note that all the other modes contributing to two-phonon scattering do not exhibit any measurable renormalization upon cooling into the SC state (see Figs. 1 and 2), thereby the 635 cm^{-1} E_{2g} boron stretching mode

is the only phonon that exhibits renormalization below the SC transition.

4. Summary

We have measured the polarization resolved Raman response as a function of temperature, field and excitation energy for MgB_2 single crystals.

The electronic scattering data revealed three superconductivity induced spectroscopic features: a clean threshold below $2\Delta_0 = 37\ \mathrm{cm}^{-1}$ corresponding to the fundamental gap, a coherence peak at $2\Delta_l = 109\ \mathrm{cm}^{-1}$ corresponding to the gap on the σ-bands FS, and the Leggett's collective mode at $\omega_L = 78\ \mathrm{cm}^{-1}$ arising from the fluctuation in the relative phase between two coupled SC condensates residing on two bands. Altogether the electronic Raman spectra show signatures for superconductivity in the clean limit for quasi-two-dimensional σ-bands and dirty limit for three-dimensional π-bands. The ratio $2\Delta_0/k_B T_c$ is only 1.2 which makes the π-band contribution to the two band superconductivity quite tenuous, in agreement with rapid suppression of the threshold frequency by a relatively weak magnetic field. The large gap shows a BCS-like temperature dependence with the $2\Delta_l/k_B T_c$ ratio of about 4 indicating a moderately strong coupling limit. The $2\Delta_l$ gap magnitude is suppressed by an external magnetic field at the rapid rate of $-15\ \mathrm{cm}^{-1}/\mathrm{T}$.

From the temperature dependence of the E_{2g} boron stretching phonon linewidth we conclude that anharmonic decay is primarily responsible for the anomalously large damping constant of this mode. For this phonon we observe a SC induced self-energy effect and estimate the electron–phonon coupling constant.

Acknowledgements

The authors thank M.V. Klein, A.A. Kuz'menko, D. van der Marel, I.I. Mazin and W.E. Pickett for valuable discussions. AM was supported by the Lucent-Rutgers Fellowship program. NDZ was supported by the Swiss National Science Foundation through NCCR pool MaNEP.

References

[1] A.Y. Liu, I.I. Mazin, J. Kortus, Phys. Rev. Lett. 87 (2001) 087005.
[2] M. Iavarone et al., Phys. Rev. Lett. 89 (2002) 187002.
[3] P. Szabó et al., Phys. Rev. Lett. 87 (2002) 137005.
[4] S. Tsuda et al., Phys. Rev. Lett. 87 (2001) 177006.
[5] S. Souma et al., Nature 423 (2003) 65.
[6] M.R. Eskildsen et al., Phys. Rev. Lett. 89 (2002) 187003.
[7] A. Perucchi et al., Phys. Rev. Lett. 89 (2002) 097001.
[8] X.K. Chen et al., Phys. Rev. Lett. 87 (2001) 157002(R).
[9] A. Goncharov et al., Phys. Rev. B 64 (2001) 100509.
[10] J.W. Quilty et al., Phys. Rev. Lett. 88 (2002) 087001.
[11] J.W. Quilty et al., Phys. Rev. Lett. 90 (2003) 207006.
[12] A.J. Leggett, Prog. Theor. Phys. 36 (1966) 901.
[13] W.-C. Wu, A. Griffin, Phys. Rev. Lett. 74 (1995) 158.
[14] For a review see: D. van der Marel, J. Supercond. 17 (2004) 559.
[15] I.I. Mazin, V. Antropov, Physica C 385 (2003) 49.
[16] T. Yildirim et al., Phys. Rev. Lett. 87 (2001) 037001.
[17] A. Shukla et al., Phys. Rev. Lett. 90 (2003) 095506.
[18] A.Q.R. Baron et al., Phys. Rev. Lett. 92 (2004) 197004.
[19] J. Karpinski et al., Supercond. Sci. Technol. 16 (2003) 221.
[20] G. Blumberg et al., Phys. Rev. B 49 (1994) 13 295.
[21] A. Mialitsin, B.S. Dennis, N.D. Zhigadlo, J. Karpinski, G. Blumberg, Phys. Rev. B 86 (2006) 020509(R).
[22] T.P. Devereaux, R. Hackl, Rev. Mod. Phys. 78 (2007) 175.
[23] A.A. Kuz'menko et al., Solid State Commun. 121 (1990) 175.
[24] V. Guritanu et al., Phys. Rev. B 73 (2006) 104509.
[25] V.P. Antropov et al., cond-mat/0107123.
[26] J. Kortus et al., Phys. Rev. Lett. 86 (2001) 4656.
[27] T. Strohm, M. Cardona, Phys. Rev. B 55 (1997) 12725.
[28] S.G. Sharapov, V.P. Gusynin, H. Beck, Eur. Phys. J. B 30 (2002) 45.
[29] H. Choi et al., Nature 418 (2002) 758.
[30] D. Daghero et al., Physica C 408–410 (2004) 353.
[31] B. Renker et al., J. Low Temp. Phys. 131 (2003) 411.
[32] M. Calandra, F. Mauri, Phys. Rev. B 71 (2005) 064501.
[33] E. Cappelluti, Phys. Rev. B 73 (2006) 140505.
[34] L. Boeri, E. Cappelluti, L. Pietronero, Phys. Rev. B 71 (2005) 012501.
[35] D. Hinks, J. Jorgensen, Physica C 385 (2003) 98.
[36] H. Choi et al., Phys. Rev. B 66 (2002) 020513.
[37] R. Osborn et al., Phys. Rev. Lett. 87 (2001) 017005.
[38] K. Bohnen, R. Heid, B. Renker, Phys. Rev. Lett. 86 (2001) 5771.
[39] A.F. Goncharov, V.V. Struzhkin, Physica C 385 (2003) 117.
[40] R. Zallen, Phys. Rev. B 9 (1974) 4485.
[41] T. Tomita et al., Phys. Rev. B 64 (2001) 092505.
[42] I. Loa, K. Syassen, Physica C 118 (2001) 279.
[43] R. Zeyher, G. Zwicknagl, Z. Phys. B 78 (2002) 479.
[44] C.R. Rodriguez et al., Phys. Rev. B 42 (1990) R2692.
[45] R. Zeyher, Phys. Rev. Lett. 90 (2003) 107002.
[46] A. Golubov et al., J. Phys. Cond. Mat. 14 (2002) 1353.